Eur. Phys. J. B **60**, 75–81 (2007)
DOI: 10.1140/epjb/e2007-00323-0

THE EUROPEAN PHYSICAL JOURNAL B

Elastic and brittle properties of the B2-MgRE (RE = Sc, Y, Ce, Pr, Nd, Gd, Tb, Dy, Ho, Er) intermetallics

Y. Wu[a] and W. Hu

Department of Applied Physics, Hunan University, Changsha 410082, China, and Materials Science and Engineering College, Hunan University, Changsha 410082, P.R. China

Received 2 March 2007 / Received in final form 25 October 2007
Published online 29 November 2007 –

Abstract. The brittle and elastic properties of the B2-MgRE (RE = Sc, Y, Ce, Pr, Nd, Gd, Tb, Dy, Ho, Er) intermetallics have been investigated using first-principles density functional calculations. The calculated equilibrium lattice constants and enthalpies of formation are in overall agreement with the available experiment and theoretical results. The related physical properties of those compounds are compared with that of ductile YCu. The Fermi energy occurs above a peak in the DOS for B2-MgRE intermetallics, whereas for ductile YCu the Fermi energy occurs near a minimum in the DOS. For B2-YCu, the partial density of states of d-states at the Fermi energy is low, while for B2-MgRE the RE d-states are partially occupied, indicating their important roles in the directional bonding for this material. The Cauchy pressure (C_{12}-C_{44}) and the ratio of bulk to shear modulus B/G are used to assess the brittle/ductile behavior of B2-MgRE and YCu compounds. It can be concluded that the B2-MgRE alloys have brittle behavior. MgSc is the most brittle, and MgHo is the least brittle amongst those alloys.

PACS. 71.15.Mb Density functional theory, local density approximation, gradient and other corrections – 71.20.Lp Intermetallic compounds – 62.20.Dc Elasticity, elastic constants

1 Introduction

Magnesium forms a wide range of ordered intermetallics with rare earth (RE) metals [1–8], such as MgRE (CsCl-type), Mg_2RE (Cu_2Mg-type or Zn_2Mg-type), Mg_3RE (BiF_3-type), Mg_5RE_{24}(α-Mn-type) and $Mg_{12}RE$ ($Mn_{12}Th$-type). Thermodynamic and stability properties of Mg-RE alloys have been investigated in the literature [7–9]. Recently, various studies [10–13] have been undertaken of the magnetic properties for some cubic (CsCl structure) rare-earth-magnesium equiatomic compounds MgRE (RE = Tb, Dy, Ho, Er, Gd, Ce). They showed that the magnetic structures which appear at low temperatures are rather complicated, resulting from exchange effects in the presence of a crystalline electric field. However, the electronic structure of intermetallic compounds of Mg with rare earth metals have received little attention, either experimentally or theoretically.

It is known that elastic properties of a solid are important because they are closely associated with various fundamental solid-state properties such as interatomic potentials, equation of state, and phonon spectra. These parameters provide a link between mechanical and dynamic behavior of a crystal. The elastic constants determine the response of the crystal to external forces, as characterized by bulk modulus, shear modulus, Young's modulus, and Poisson's ratio, and obviously play an important role in determining the strength, brittleness/ductility, and hardness of materials. To understand physical properties of these compounds and provide significant information with respect to application and design of Mg-rare earth alloys, it is necessary to study further the electronic structure and elastic constants of these compounds. In the present paper, we investigate systemically the electronic and brittle behavior for B2-MgRE (RE = Sc, Y, Ce, Pr, Nd, Gd, Tb, Dy, Ho, Er) via first-principles calculations. At the same time, the related physical properties of these compounds are compared to that of YCu and NiAl. In 2003, Gschneidner et al. [14,15] reported a family of ductile intermetallic compounds such as YAg, YCu, DyCu and CeAg, which possess unusually high room temperature ductility. By comparison, it can be found that there is an important difference between B2-MgRE and YCu. Moreover, the mechanism is analyzed from an electronic structural point of view.

[a] e-mail: winwyr@126.com

2 Computational details

The local density approximation (LDA) to density function theory embodied in the Vienna ab initio simulation package (VASP) [16] is employed in the present study. Exchange and correlation energies are treated using the generalized gradient approximations (GGA) of Perdew and Wang (PW91) [17]. Projector augmented wave (PAW) functions [18] are used. The energy cut-off is chosen to be 400 eV. Brillouin-zone integrations were performed using Monkhorst and Pack [19] k-point meshes, the k-meshes for B2-MgRE(RE = Sc, Y, Ce, Pr, Nd, Gd, Tb, Dy, Ho, Er) are 13×13×13 for energy and lattice constants, 21×21×21 is selected for DOS calculations.

The elastic constants [20,21] C_{ijkl} (where i, j, k, l refer to Cartesian components) are defined by means of a Taylor expansion of the total energy of the system, E (V, e), with respect to a small strain e of the lattice (V is the volume of system). The distortion of the lattice is expressed by defining a strain tensor, ε, such that the primitive lattice vectors a_i ($i = 1, 2, 3$), are transformed to the new vectors

$$\begin{pmatrix} a_1' \\ a_2' \\ a_3' \end{pmatrix} = \begin{pmatrix} a_1 \\ a_2 \\ a_3 \end{pmatrix} \cdot (I + \varepsilon) \tag{1}$$

where I is a 3×3 identity matrix, ε is the strain tensor. This links with the strain vector e by

$$\varepsilon = \begin{pmatrix} e_1 & \frac{e_6}{2} & \frac{e_5}{2} \\ \frac{e_6}{2} & e_2 & \frac{e_4}{2} \\ \frac{e_5}{2} & \frac{e_4}{2} & e_3 \end{pmatrix}. \tag{2}$$

The Taylor expansion of the total energy can be written as

$$E(V, e_i) = E(V_0, 0) - P(V_0)\Delta V + \frac{V_0}{2} \sum_{i,j} C_{ij} e_i e_j + \mathrm{O}[e_i^3]. \tag{3}$$

Here V_0 is the volume of the undistorted lattice, $P(V_0)$ is the pressure of the undistorted lattice at volume V_0, ΔV is the change in the volume of the lattice due to the strain in equation (3). The pressure is neglected in our present study, so the value of $P(V_0)$ in equation (3) is zero. Therefore equation (3) can be written as

$$\Delta E = E(V, e_i) - E(V_0, 0) = \frac{V_0}{2} \sum_{i,j} C_{ij} e_i e_j + \mathrm{O}[e_i^3] \tag{4}$$

where $\mathrm{O}[e^3]$ indicates that the neglected terms in the polynomial expansion are cubic and a higher power of the e_i.

For cubic phases there are three independent elastic constants, C_{11}, C_{12} and C_{44}. The shear modulus $C' = (C_{11} - C_{12})/2$, bulk modulus B, and C_{44} are calculated from volume-conserving orthorhombic strain $e = (\delta, \delta, (1+\delta)^{-2} - 1, 0, 0, 0)$, hydrostatic pressure $e = (\delta, \delta, \delta, 0, 0, 0)$ and tri-axial shear strain $e = (0, 0, 0, \delta, \delta, \delta)$, respectively [21]. So C_{44} can be calculated from

$$\frac{\Delta E}{V_0} = \frac{3}{2} C_{44} \delta^2 \tag{5}$$

C' is given by

$$\frac{\Delta E}{V_0} = 6C'\delta^2 + O(\delta^3) \tag{6}$$

B can be obtained by

$$\frac{\Delta E}{V_0} = \frac{9}{2} B \delta^2. \tag{7}$$

Then C_{11} and C_{12} are hence given by

$$C_{11} = \frac{3B + 4C'}{3}, \quad C_{12} = \frac{3B - 2C'}{3}. \tag{8}$$

Using the above-mentioned strains, we have calculated a series of $\Delta E/V_0 \sim \delta$ data. These data were then fitted using a quadratic polynomial and the relevant elastic constant was obtained from the coefficient of the quadratic term in the corresponding equations (5)–(9).

The single-crystal shear moduli for the {100} plane along the [010] direction and for the {110} plane along the $[1\bar{1}0]$ direction are simply given by $G_{\{100\}} = C_{44}$ and $G_{\{110\}} = (C_{11} - C_{12})/2$, respectively. The shear constant C_{44} is associated with a tetragonal deformation and its size reflects the degree of stability of the crystal with respect to a tetragonal shear. In addition, since C_{11}, C_{12} and C_{44} are a complete set of elastic constants for a cubic system, shear modulus G, Young's modulus E, Poisson's ratio ν, and shear anisotropy factor A, can be calculated from the following relations:

$$G = \frac{3C_{44} + C_{11} - C_{12}}{5} \tag{9}$$

$$E = \frac{9BG}{3B + G} \tag{10}$$

$$v = \frac{C_{12}}{C_{11} + C_{12}} \tag{11}$$

$$A = \frac{2C_{44}}{C_{11} - C_{12}}. \tag{12}$$

3 Results and discussions

3.1 Lattice parameter and enthalpy of formation

In order to obtain the lattice parameter of B2-MgRE, a series of $E \sim a$ data are calculated; the results are shown in Figure 1, as an example of B2-MgPr. The fitted lattice parameters of B2-MgRE are listed in Table 1 together with the available experimental [7,8,22,23,26] and other theoretical results [24,25,27]. Our calculated results for the equilibrium lattice constants are within 1% of the experimental values. The calculated enthalpy of formation for MgPr, MgNd, MgGd and MgY are in good agreement with the experimental and other theoretical values, those of MgSc, MgTb and MgHo agree well with the other theoretical results. The calculated formation enthalpy for MgCe, which shows the largest discrepancy with experiment, is in good agreement with the Miedema results of

Table 1. The calculated lattice parameter and enthalpy of formation for B2-MgRE, as well as the experimental [7,22,23,26,27] and other theoretical results [24,25,28].

Mg-RE	Lattice parameter (Å)		Enthalpy of formation (eV)		
	This study	Experiment[a]	This study	Experiment	Other theory
MgCe	3.917	3.912	–0.126	–0.565[b]	–0.282[c], –0.135[d]
MgPr	3.901	3.877	–0.134	–0.179[e]	–0.125[d]
MgNd	3.872	3.860	–0.158	–0.154[f]	–0.127[d]
MgGd	3.811	3.818	–0.102	–0.181[f]	–0.121[d], –0.179[g]
MgSc	3.593	3.597	–0.041	-	–0.082[d]
MgY	3.796	3.796	–0.110	–0.131[h]	–0.125[d]
MgTb	3.781	3.781	–0.093	-	–0.116[d]
MgHo	3.771	3.770	–0.074	-	–0.114[d]
MgDy	3.765	3.759	–0.083	–0.125[f]	–0.116[d]
MgEr	3.738	3.734	–0.064	–0.22[f]	–0.110[d]

[a] Reference [22]; [b] reference [23]; [c] reference [24]; [d] reference [25]; [e] reference [26]; [f] reference [27]; [g] reference [28]; [h] reference [7]

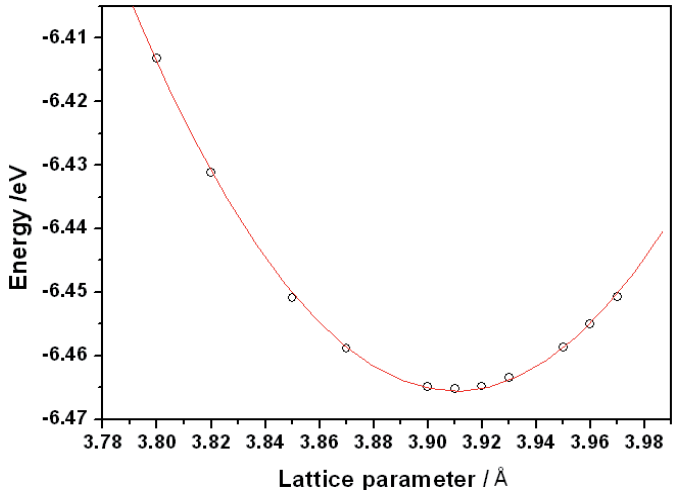

Fig. 1. Calculated total energy as a function of lattice parameter for MgPr.

–0.135 eV [25]. In general, a good agreement is shown between the calculated results for B2-MgRE and the experimental and other theoretical values, showing that the parameters from the first-principles VASP calculation in the present study are valid. This validates the calculation of electronic structure and elastic constants.

3.2 Electronic structure

The density of states (DOS) of B2-MgRE, YCu and NiAl are shown in Figure 2(a-l). It can obviously be seen that the DOS of MgRE is quite different from that of YCu, showing a difference in the bonding as well. For MgRE and NiAl, the Fermi energy occurs above a peak in the DOS; the bonding states are full, and the filling of the anti-bonding states is sensitive to deviations in the local structure that affect the Fermi energy. In contrast, for ductile YCu the Fermi energy occurs near a minimum in the DOS, and the bonding states are only partially full. Thus, the bonding is relatively insensitive to local distortions. Moreover, for all 10 MgRE intermetallics, the magnitude of the DOS at Fermi energy for MgEr is the largest, and MgCe is the smallest. Therefore, MgRE intermetallics may be brittle, while YCu is ductile, which is in accordance with previous studies [14,15]. The typical MgY partial densities of states were shown in Figure 3, that of YCu also shown in Figure 3. For YCu, the largest contribution comes from Y and Cu d-states to the density of states, and the density of d-states at the Fermi energy is low. In contrast, for MgY, the structures observed in the whole energy range are mainly Y d-states, the Y d-states partially occupied, displaying their important role in the directional bonding for this material. In addition, the partial DOS given in Figure 3 shows that the Y d and Y p states are mixed with Mg p states at the Fermi energy, indicating large Y(d and p)-Mg(p) hybridization.

3.3 Elastic constants

Figure 4 presents, as a typical example of the series, the energy $\Delta E(V_0, \delta)$ versus three different strain δ for MgPr. The bulk modulus B, elastic constants C_{11}, C_{12} and C_{44}, are then obtained by means of polynomial fits. The calculated elastic constants C_{11}, C_{12}, C_{44}, bulk modulus B, and shear modulus $G_{\{110\}}$ are listed in Table 2. For YCu, the calculated results are in good agreement with the experimental values [15]. No elastic constants have been reported experimentally and theoretically for all MgRE intermetallics. It is noticeable that for all MgRE and YCu intermetallics, all elastic constants are larger than zero, namely, $C_{44} > 0$, $C_{11} > 0$, and $C_{11} > C_{12}$, which is in accordance with the stability condition for a crystal [28], implying that those intermetallics are elastically stable. For all 10 MgRE compounds, shear modulus $G_{\{100\}} \gg G_{\{110\}}$, indicating that it is easier to shear on the {110} plane along the $[1\bar{1}0]$ direction rather than on the {100} along the [010] direction. The shear modulus $G_{\{100\}}$ and $G_{\{110\}}$ of MgSc has a maximum. This phenomenon does not occur for YCu, which is also a difference between MgRE

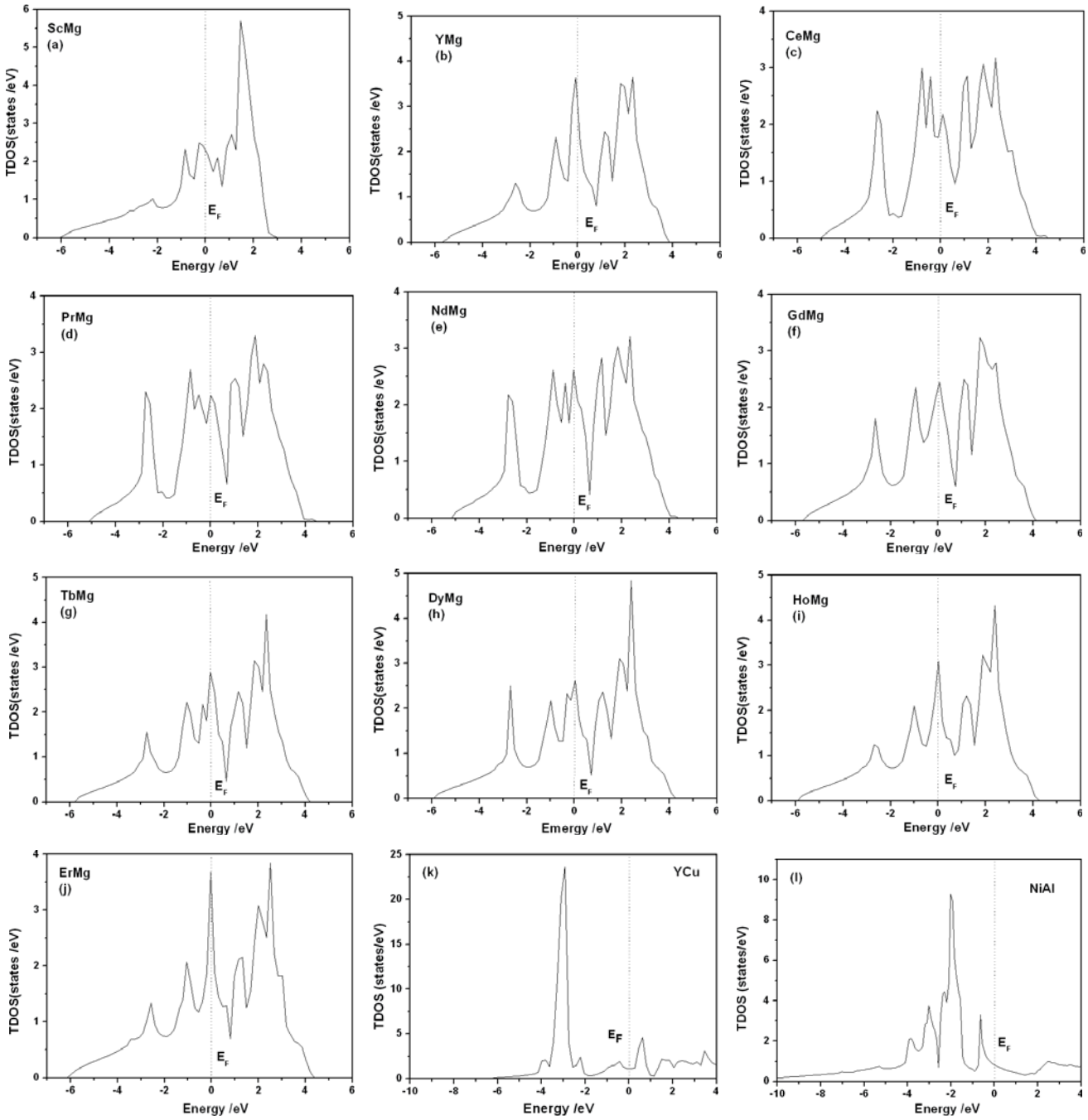

Fig. 2. The total density of states for: (a)–(j) MgRE; (k)YCu; (l) NiAl. The Fermi energy is shifted to zero.

and ductile YCu. In addition, it can be seen that the bulk modulus B of MgSc is the largest among the 10 B2-MgRE alloys, indicating the highest strength for MgSc.

Table 3 gives the shear modulus G, Young's modulus E, B/G, Poisson's ratio ν, the shear anisotropy factor A and Cauchy pressure $C_{12} - C_{44}$ for MgRE and YCu, as well as experimental values [15] for YCu. It is known that the hardness and strength of materials are related to their elastic moduli, such as the Young's modulus E, bulk modulus B and the shear modulus G [29]. Although the relationship between hardness and the modulus are not identical for different materials, the general trend is, the larger the modulus, the harder the material. Therefore, for all MgRE compounds, MgSc is expected to be the hardest due to its largest modulus. It is noticeable that all MgRE compounds have a relatively high shear anisotropy factor, showing anisotropy behavior, while the shear anisotropy factor of YCu is close to 1, indicating a more isotropic behavior. For Cauchy pressure, Pettifor [30] has suggested that it could be used to describe the angular character of atomic bonding in metals and compounds. If the bonding is more metallic in character,

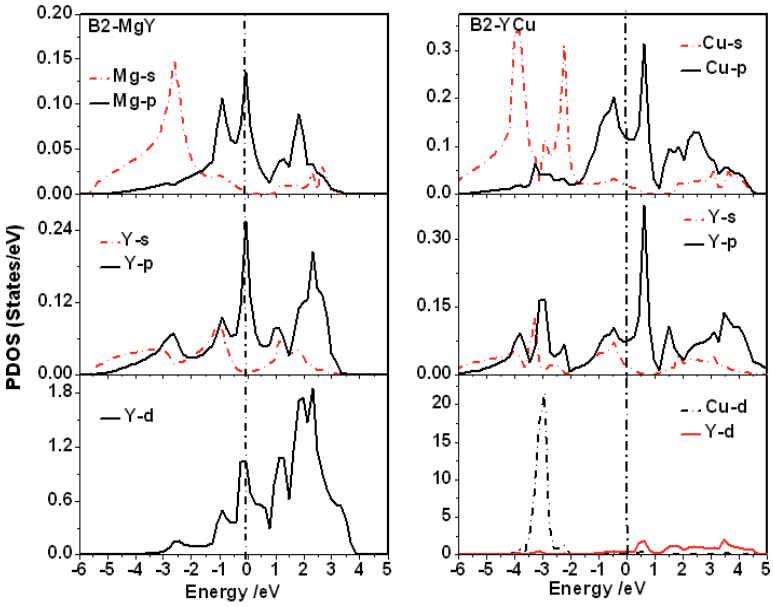

Fig. 3. Partial density of states for: (left) MgY; (right) YCu.

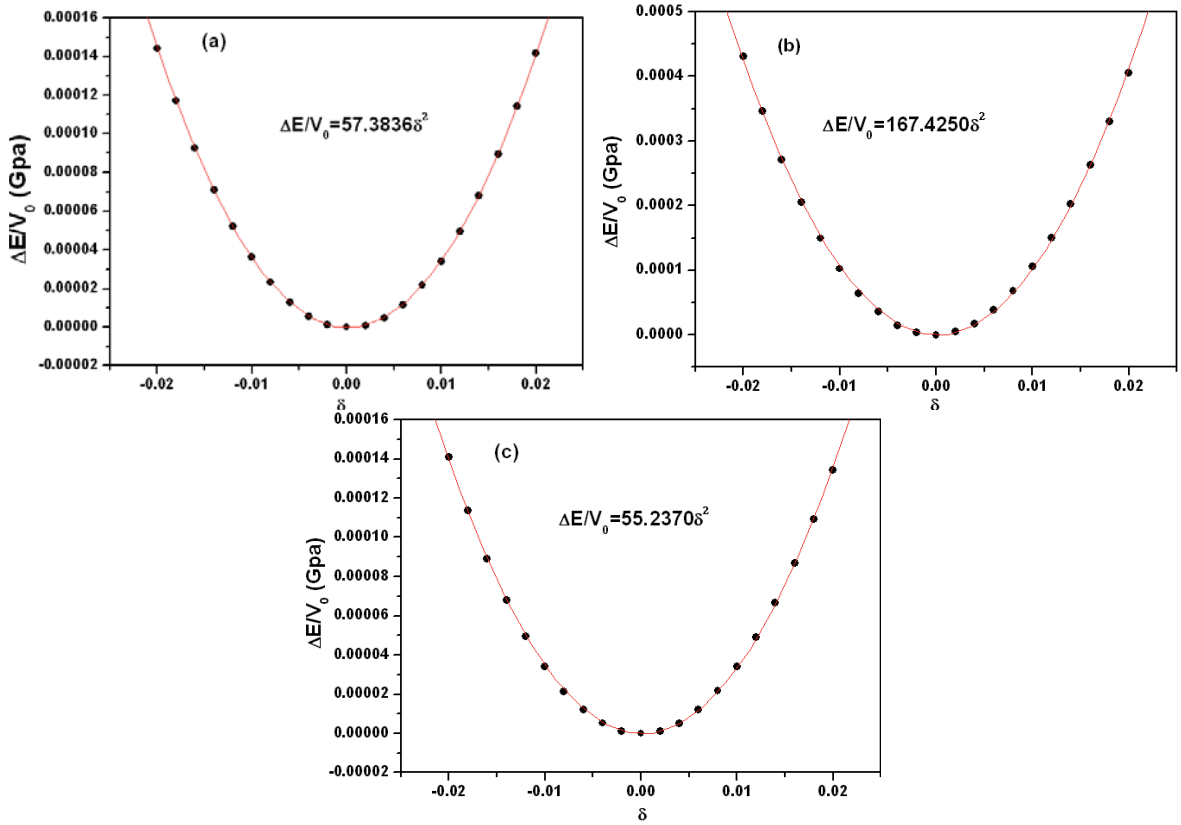

Fig. 4. The energy $\Delta E(V_0, \delta)$ versus three different strain δ for MgPr intermetallics: (a) C_{44}; (b) bulk modulus B; (c) shear modulus $C' = (C_{11} - C_{12})/2$.

the Cauchy pressure will be positive. A negative Cauchy pressure, however, requires an angular or directional character in the bonding. The more negative the Cauchy pressure, the more directional and lower mobility the bonding. For example, for ductile materials such as Ni and Al, the Cauchy pressures have positive values, while for brittle semiconductors such as Si, the Cauchy pressure is negative. In Table 3 the Cauchy pressures have positive values for ductile YCu compounds, while the Cauchy pressure is negative for MgRE intermetallics. This explains why the 10 B2-MgRE intermetallics exhibit brittle behavior, whereas YCu is ductile. The Cauchy pressure of MgSc is the most negative among the 10 MgRE alloys, indicating the most directional and brittle behavior.

Table 2. The calculated elastic constants, bulk modulus B and shear modulus $G_{\{110\}}$ for MgRE and YCu, as well as experimental values [15] for YCu. The unit is GPa.

	C_{11}	C_{12}	C_{44}	$G_{\{110\}}$	B
MgSc	70.77	43.11	55.65	13.83	52.33
MgY	53.37	36.39	39.05	8.49	42.06
MgCe	49.10	30.07	35.98	9.52	36.41
MgPr	49.96	30.80	36.80	9.58	37.20
MgNd	51.73	32.15	38.69	9.79	38.67
MgGd	55.09	35.84	42.02	9.63	42.26
MgTb	53.32	36.18	39.82	8.57	41.89
MgHo	50.00	37.15	37.87	6.43	41.43
MgDy	51.86	37.57	38.35	7.15	42.32
MgEr	52.16	41.03	42.09	5.57	43.25
YCu	117.7	47.2	36.1	35.25	70.7
Exp	113.4	48.4	32.3	32.5	70.1

Table 3. Calculated shear modulus G, Young's modulus E, B/G, Poisson's ratio ν, the shear anisotropy factor A and Cauchy pressure $C_{12} - C_{44}$ for MgRE and YCu, as well as experimental values [15] for YCu.

	G(GPa)	E(GPa)	B/G	ν	A	C_{12}-C_{44}(GPa)
MgSc	38.92	93.57	1.344	0.379	4.024	−12.54
MgY	26.83	66.37	1.568	0.405	4.600	−2.66
MgCe	25.39	61.81	1.434	0.380	3.781	−5.91
MgPr	25.91	63.09	1.436	0.381	3.841	−6.00
MgNd	27.13	65.96	1.425	0.383	3.952	−6.54
MgGd	29.06	70.93	1.454	0.394	4.366	−6.18
MgTb	27.32	67.32	1.533	0.404	4.646	−3.64
MgHo	25.29	63.05	1.638	0.431	5.894	−0.72
MgDy	25.87	64.47	1.636	0.420	5.367	−0.78
MgEr	27.48	68.03	1.574	0.440	7.563	−1.06
YCu	35.76	91.80	1.977	0.286	1.02	11.1
Exp	32.38	84.18	2.165	0.299	0.99	16.1

Pugh [31] has proposed a simple relationship that links empirically the plastic properties of metals with their elastic moduli by B/G. If $B/G > 1.75$, the material behaves in a ductile manner, otherwise a brittle manner, as recently demonstrated in a study of brittle versus ductile transition in intermetallic compounds from first principles calculations [30,32]. The higher the value of B/G, the more ductile the material would be. The B/G ratio of MgRE alloys is less than 1.75. Therefore, all MgRE compounds are brittle, MgSc the most brittle, and MgHo the least brittle. This also demonstrates that B2-MgRE intermetallics behave in a brittle manner. For Poisson's ratio, it has been noted [14,33] that the brittle B2 intermetallics have high Poisson's ratios ν, >0.35 such as FeAl ($\nu = 0.37$) and NiAl ($\nu = 0.41$), while ductile B2 intermeallics have Poisson's ratios of ∼0.3. From the Table 3, it can be seen that the Poisson's ratios of B2-MgRE intermetallics are larger than 0.35. Therefore, B2-MgRE compounds have brittle behavior, while YCu is ductile, which is agreement with experiment [14].

4 Conclusions

Ab initio density functional theory calculations have been performed to study the electronic and elastic properties of B2-MgRE (Sc, Y, Ce, Pr, Nd, Gd, Tb, Dy, Ho, Er) intermetallics. The calculated equilibrium lattice constants and enthalpies of formation are in overall agreement with the available experiment and theoretical values. The DOS of B2-MgRE and NiAl compounds is different from that of YCu. For MgRE and NiAl, the Fermi energy occurs above a peak in the DOS, while for ductile YCu the Fermi energy occurs near a minimum in the DOS, indicating B2-MgRE

intermetallics may be brittle. This is because B2-MgRE and YCu show an important difference in the bonding. For YCu, the density of d-states at the Fermi energy is low. In contrast, for B2-MgRE, the RE d-states are partially occupied, indicating their important roles in the directional bonding for these materials. Furthermore, the B2-MgRE alloys have a relatively high shear anisotropy factor. The Cauchy pressure of YCu is positive, while that of B2-MgRE is negative. The B/G ratio, proposed by Pugh to provide a simple rule for predicting ductility/brittleness, is smaller than 1.75 for B2-MgRE, implying brittle behavior. Accordingly, MgSc is the most brittle, and MgHo the least brittle among 10 B2-MgRE compounds, as well as MgSc the most hardness/strength.

This work is financially supported by the National Natural Science Foundation under contract Nos. 50371026, 50571036 and 50671035.

References

1. S. Delfino, A. Saccone, R. Ferro, Metall. Trans. A **21**, 2109 (1990)
2. A. Saccone, A.M. Cardinale, S. Delfino, R. Ferro, Intermetallics **1**, 151 (1993)
3. A. Saccone, S. Delfino, D. Macciò, R. Ferro, J. Phase Equil. **14**, 479 (1993)
4. A. Saccone, S. Delfino, D. Macciò, R. Ferro, Z. Metallkd. **82**, 568 (1991)
5. A. Saccone, S. Delfino, D. Macciò, R. Ferro, J. Phase Equil. **14**, 280 (1993)
6. A. Saccone, S. Delfino, D. Macciò, R. Ferro, Metall. Trans. A **23**, 1005 (1992)
7. C. Colinet, J. Alloys Comp. **225**, 409 (1995)
8. J.E. Pahlman, J.F. Simth, Metall. Trans. **3**, 2423 (1972)
9. Hu Wangyu, Xu Huaide, Shu Xiaolin et al., J. Phys. D: Appl. Phys. **33**, 711 (2000)
10. M. Belakhovsky, J. Chappert, D. Schmitt, J. Phys. C: Solid State Phys. **10**, L493 (1977)
11. S.E. Luca, M. Amara, R.M. Galera, J.F. Berar, J. Phys.: Condens. Matter **14**, 935 (2002)
12. M. Deldem, M. Amara, R.M. Galera, P. Morin, D. Schmitt, B. Ouladdiaf, J. Phys.: Condens. Matter **10**, 165 (1998)
13. R. Aleonard, P. Morin, J. Pierre, D. Schmitt, J. Phys. F: Metal Phys. **6**, 1361 (1976)
14. K. Gschneidner Jr, A. Russell et al., Nature Materials **2**, 587 (2002)
15. J.R. Morris, Yiying Ye, Yong-Bin Lee et al., Acta Materialia **52**, 4849 (2004)
16. G. Kress, J. Furthmuller, Phys. Rev. B **54**, 11169 (1996)
17. J.P. Perdew, Y. Wang, Phys. Rev. B **45**, 13244 (1992)
18. P.E. Blöchl, Phys. Rev. B **50**, 17953 (1994)
19. M. Methfessel, A.T. Paxton, Phys. Rev. B **40**, 3616 (1989)
20. D. Iotova, N. Kioussis, S.P. Lim, Phys. Rev. B **54**, 14413 (1996)
21. S.Q. Wang, H.Q. Ye, J. Phys.: Condens. Matter **15**, 5307 (2003)
22. P. Villars, L.D. Calvert, *Pearson's Handbook of Crystallographic Data for Intermetallic Phases* (ASM, Metals Park, oH, 1985)
23. W. Biltzm, H. Piper, Z. Anorg. Chem. **134**, 13 (1924)
24. G. Suzana, T. Jantzen, Thermochimica Acta **314**, 23 (1998)
25. O. Yifang, Z. Bangwei, L. Shuzhi, Jin Zhangpeng, Rare Metal Mater. Eng. **24**, 32 (1995)
26. G. Canneri, A. Rossi, Gazz. Chim. Ital. **63**, 182 (1933)
27. G. Cacciamani, A. Saccone, G. Borzone, S. Delfino, R. Ferro, Thermochimica Acta **199**, 17 (1992)
28. J.F. Nye, *Physical Properties of Crystals* (Clarendon Press, Oxford, 1964)
29. I.N. Frantsevich, F.F. Voronov, S.A. Bokuta, *Elastic Constants and Elastic Moduli of Metals and Insulators*, edited by I.N. Frantsevich (Naukova Dumka, Kiev, 1983), pp. 60–180
30. D.G. Pettifor, Mater. Sci. Tech. **8**, 345 (1992)
31. S.F. Pugh, Philos. Mag. **45**, 823 (1954)
32. K. Chen, L.R. Zhao, J. Rodgers, J.S. Tse, J. Phys. D: Appl. Phys. **36**, 2725 (2003)
33. M.H. Yoo, T. Takasugi, S. Hanada, O. Izumi. S. Mater. Trans. JIM **31**, 435 (1990)